Computations of the Response of a Wave Spectrum to a Sudden Change in Wind Direction

I. R. YOUNG

Department of Civil Engineering, Australian Defence Force Academy, Canberra, Australia

S. HASSELMANN AND K. HASSELMANN

Max-Planck-Institute for Meteorology, Hamburg, Federal Republic of Germany

(Manuscript received and in final form 2 September 1986)

ABSTRACT

The response of a wind-sea spectrum to a step function change in wind direction is investigated theoretically for a sequence of direction changes ranging from 30° to 180°, in increments of 30°. Two spectral energy balance models are used: the model EXACT-NL, in which the nonlinear transfer is represented exactly, and the model 3G-WAM, in which the nonlinear transfer is approximated by the discrete interaction parameterization. In both models the input and dissipation source functions are taken from the energy balance proposed by Komen et al. The operational model 3G-WAM reproduces fairly closely the EXACT-NL results. For wind direction changes less than 60°, the wind-sea direction adjusts smoothly. The high-frequency components relax more rapidly to the new wind direction than the low-frequency components. The computed relaxation rates are generally consistent with the analysis of measured directional spectra by D. E. Hasselmann et al. and Allender et al. However, the relaxation rate is found to be a function of wind speed as well as frequency. For wind direction changes greater than 60°, a second, independent wind-sea spectrum is generated in the new wind direction, while the old wind-sea gradually decays as swell.

1. Introduction

In recent years a fairly consistent picture of the spectral energy balance of ocean waves has emerged. The evolution of the spectrum in both space and time results from a combination of several physical processes which are generally of comparable magnitude: the propagation of energy, atmospheric input due to wind forcing, the dissipation of energy due to wave breaking or white-capping, and the transfer of energy between spectral components due to resonant nonlinear interactions. The rather sensitive balance between these processes has been studied in detail for fetch limited wave growth and fully developed spectra (e.g., Mitsuyasu, 1968a, 1969; Komen et al., 1984). However, relatively few studies have been carried out for the more complex wind fields that are often encountered in nature. In particular, little detailed information is available on the response of the wave spectrum to rapid changes in wind direction. A better understanding of the spectral balance in such situations is of considerable practical importance for reliable wave predictions for strong frontal systems, hurricanes, polar lows, and other intense, relatively small-scale storm events.

A qualitative picture of the spectral response to a sudden wind shift has been obtained from the analysis of field observations by D. Hasselmann et al. (1980), Günther et al. (1981) and Allender et al. (1983). All authors report a strong frequency dependence of the directional relaxation, the high-frequency waves aligning rather quickly with the wind direction, whereas the low-frequency wind-sea components tend to lag behind the wind direction and may take several hours to align completely with the wind. Low-frequency swell, as expected, shows no response to wind direction changes.

Formally, spectral growth is described by the energy or radiative transfer equation, in which these physical processes are represented as individual source terms. All three source functions may be expected to affect the directional relaxation process: the energy input by the wind into the new wind sea, the attenuation of the old wind sea, and nonlinear interactions, which transfer energy from the old sea to the developing new wind sea. The SWAMP (1985) study, however, in which a number of numerical wave prediction models were intercompared, revealed large differences in the way in which different models treated the energy balance in turning wind situations. This was attributed to the unsatisfactory representation of the source terms in complex sea conditions and to the arbitrariness with which these shortcomings were overcome in the models by additional assumptions.

The main problem in handling complex wind seas in present wave models stems from the difficulty of accurately representing the nonlinear interaction term. The exact computation of the full Boltzmann interaction integral (Hasselmann, 1961) is too time consuming for incorporation in routine two-dimensional

wave models. The problem is generally resolved by either neglecting the nonlinear terms altogether and adopting largely empirical linear growth relations (first generation models) or by using relatively simple parameterized descriptions for the effect of the nonlinear transfer on the spectrum (second generation models). A difficulty of this approach has been that the numerical representation of the wave spectrum generally has significantly more degrees of freedom than the parametric representation of the nonlinear source term. Consequently, the correct spectral balance cannot be maintained by the models throughout the spectrum if all of the degrees of freedom are allowed to evolve freely. In practice, this is overcome in present second generation wave models by restricting the shape of the spectrum, normally in accordance with empirical relations obtained for uniform wind, fetch-limited wave growth. Although such models perform quite well for the simple wave fields for which they were calibrated, they are not sufficiently flexible to handle the complex seas resulting from a sudden wind shift (cf. SWAMP, 1985). More recent third generation wave models (S. Hasselmann et al., 1987) resolve these difficulties by introducing operator parameterization of the nonlinear transfer that contain the same number of degrees of freedom as used to describe the spectrum.

In this paper we investigate the spectral response to a sudden shift in wind direction by numerical experiments with both a third generation wave model, 3G-WAM, and a "calibration" model EXACT-NL based on a full representation of the nonlinear source term (Hasselmann and Hasselmann, 1984). The incorporation of exact computations of the nonlinear transfer in a numerical wave model has become feasible through the development of more efficient integration methods (Hasselmann and Hasselmann, 1985) and, of course, faster computers. Nevertheless, the model EXACT-NL can still be integrated at acceptable costs only with respect to a single variable (in our case, duration). The remaining source terms of both models are identical and are taken from the energy balance study of Komen et al. (1984). Details of the computational procedures and parameterizations are given in Hasselmann and Hasselmann (1985) and S. Hasselmann et al. (1985). The model results are compared against each other and with field data.

2. The energy balance equation

The spectral evolution of deep-water ocean waves is described by the energy balance equation

$$\frac{\partial F}{\partial t} + c_g \nabla F = S_{\text{in}} + S_{\text{nl}} + S_{\text{dis}} \tag{2.1}$$

where $F = F(f, \theta; \underline{x}, t)$ denotes the two-dimensional directional frequency spectrum, the terms of the left-hand side represent the temporal accumulation of energy and the propagation of energy at the wave group velocity c_g, and the source terms on the right-hand side represent the wind input, nonlinear wave–wave interaction and dissipation, respectively.

In the model EXACT-NL (also referred to for brevity as the "full" model), the exact Boltzmann integral representation of the nonlinear transfer is computed. The model is identical to that proposed by Komen et al. (1984) (it differs in details of the input and dissipation source functions from the original model EXACT-NL of Hasselmann and Hasselmann, 1985). The third generation operational model 3G-WAM ("parametrical model") differs from the full model only in that the exact expression for S_{nl} is replaced by the discrete interaction approximation of Hasselmann et al. (1985).

The wind input for both models is based on the expression proposed by Snyder et al. (1981), which is reformulated in terms of the friction velocity, u_* rather than the wind speed at 5 m height. Arguments in favor of this form of scaling have been put forward, e.g., by Miles (1959), Pierson (1964), Mitsuyasu and Honda (1982), Janssen and Komen (1984) and Komen et al. (1984). Adopting this scaling and a drag coefficient $c_5 = 1.28 \times 10^{-3}$ (appropriate for the wind speeds encountered by Snyder et al., cf. Komen et al., 1984), Snyder's relation becomes

$$S_{\text{in}}(f, \theta) = \max\left\{0, 0.25 \frac{\rho_a}{\rho_w}[28(u_*/c)\cos\phi - 1]\omega F(f, \theta)\right\} \tag{2.2}$$

where ρ_a and ρ_w represent the densities of air and water, respectively, c is the phase speed of waves with frequency f, $\omega = 2\pi f$ and ϕ is the angle between the wind vector and the wave propagation direction. For waves propagating at angles greater than 90° to the wind, Eq. (2.2) states that there is neither growth nor decay. This is consistent with the laboratory experiments of Young and Sobey (1985), which showed that wave decay for opposing winds is quite small and for practical purposes can be assumed equal to zero.

The second source term, S_{nl}, describes the nonlinear energy transfer between waves due to third-order resonant interactions and is given by the Boltzmann integral expression (Hasselmann, 1961)

$$S_{\text{nl}}(\underline{k}) = \omega \int d\underline{k}_1 d\underline{k}_2 d\underline{k}_3 \sigma(\underline{k}_1, \underline{k}_2, \underline{k}_3, \underline{k}) \times \delta(\underline{k}_1 + \underline{k}_2 - \underline{k}_3 - \underline{k})\delta(\omega_1 + \omega_2 - \omega_3 - \omega) \times [n_1 n_2 (n_3 + n) - n_3 n (n_1 + n_2)] \tag{2.3}$$

where the action density $n(\underline{k}) = F(\underline{k})/\omega$, $n_i = n(\underline{k}_i)$ and for deep water $\omega = (gk)^{1/2}$. The symmetrical kernel σ represents a rather complex net scattering coefficient.

Equation (2.3) has been evaluated numerically by several authors using standard integration techniques (Hasselmann, 1963; Sell and Hasselmann, 1972; Webb, 1978; Masuda, 1980). The extensive computation time

required for such exact integrations has stimulated the investigation of various approximations. Narrow-peak expansions (Longuet-Higgins, 1976; Fox, 1976; Dungey and Hui, 1979) reproduce many of the qualitative features of the transfer but are not applicable for the complex seas encountered in the present study. Similar limitations apply to the local interaction approximation considered by Hasselmann et al. (1985). Accordingly, an exact integration technique was used that takes advantage of the symmetry properties of the integrand by introducing symmetric integration variables (Hasselmann and Hasselmann, 1985). Additional savings were achieved in production runs by precomputing the integration grid and the interaction coefficients and filtering out unimportant regions of the phase space. Applications of this technique to a variety of spectral shapes have been presented by Hasselmann and Hasselmann (1981) and Young et al. (1985). Although the computations are still too time consuming for incorporation in a full space–time dependent wave model, the model EXACT-NL could be integrated with respect to a single variable, either fetch or (in the present application) duration, at acceptable expense.

With both S_{in} and S_{nl} prescribed, the only freely adjustable source function is the remaining term S_{dis}. Komen et al. (1984) have investigated the form of dissipation required to yield fetch-limited wave growth in reasonable agreement with observation and, in particular, a stationary asymptotic spectrum similar to the Pierson–Moskowitz (Pierson and Moskowitz, 1964) spectrum. The best agreement was achieved with a dissipation term given by

$$S_{dis}(f,\theta) = -3.33\times 10^{-5}\bar{\omega}\left(\frac{\omega}{\bar{\omega}}\right)^2\left[\frac{\hat{\alpha}}{\hat{\alpha}_{PM}}\right]^2 F(f,\theta) \quad (2.4)$$

where $\hat{\alpha}$ is an integral wave-steepness parameter

$$\hat{\alpha} = \epsilon\bar{\omega}^4/g^2$$

defined in terms of the mean frequency

$$\bar{\omega} = \epsilon^{-1}\int F(f,\theta)\omega df d\theta$$

and energy

$$\epsilon = \int F(f,\theta) df d\theta$$

g is the gravitational acceleration and $\hat{\alpha}_{PM} = 4.57 \times 10^{-3}$ is the theoretical value of $\hat{\alpha}$ for the Pierson–Moskowitz spectrum. The general structure of Eq. (2.4) (linearity in F, square law dependence on ω) follows from rather general assumptions for any nonlinear process, such as white-capping, which is small-scale, local and "weak-in-the-mean" (Hasselmann, 1974).

3. Numerical solution

For the case of duration limited growth of a homogenous wave field, Eq. (2.1) simplifies to

$$\frac{\partial F}{\partial t} = S_{tot} \quad (3.1)$$

where $S_{tot} = S_{in} + S_{nl} + S_{dis}$. Equation (3.1) was integrated numerically using a straightforward first-order forward difference scheme with a dynamically adjusted time step. To maintain an acceptable time step, the spectrum was predicted explicitly only in the frequency range $f \leqslant 3f_p$, where f_p is the frequency of the spectral peak. For $f > f_p$, an f^{-5} high-frequency tail was added. (An f^{-4} tail may have been more appropriate for this frequency range, cf. Toba, 1973, and other more recent investigations. However, the results were not sensitive to the exact form of the tail, which contains less than 10% of the total wave energy.)

A simple first-order integration scheme was considered adequate, since the time step was determined by the rapidly responding high-frequency region of the spectrum close to the $3f_p$ cut-off. The time step was therefore very small relative to the dynamical time scales of the energetically relevant wave components near the spectral peak.

A unidirectional, homogeneous, wind field with $u_* = 0.357$ m s^{-1} (corresponding to a wind velocity of the order of 10 m s^{-1}) was used as the driving field. However, as all results are presented later in nondimensional form by scaling with respect to u_* and g, the value of u_* is, in fact, immaterial.

Since S_{in} contains no Phillips (1957) type term to trigger growth, a JONSWAP spectrum with $\alpha = 0.018$, $\gamma = 3.3$ and $f_p = 0.4$ was taken as the initial spectrum, with a spreading function of the form proposed by Hasselmann et al. (1980). The choice of this initial spectrum is not critical, as it is quickly modified by the nonlinear interactions.

The spectrum was allowed to grow under the action of the wind until the peak frequency, f_p, reached $2f_{PM}$, where

$$f_{PM} = 0.14g/U_{19.5} \quad (3.2)$$

represents the peak frequency of the Pierson–Moskowitz spectrum for a given wind speed $U_{19.5}$. In terms of u_* Eq. (3.2) can be written

$$f_{PM} = 0.0056g/u_*. \quad (3.3)$$

(In transforming the Pierson–Moskowitz relations into equivalent u_* dependent formulae, a larger drag coefficient, $c_{19.5} = 1.6 \times 10^{-3}$, was used than the drag coefficient $c_5 = 1.28 \times 10^{-3}$ applied in the transformation of Snyder et al.'s input source function, as the Pierson–Moskowitz data correspond to higher wind speed than Snyder et al.'s data; cf. Komen et al., 1984).

Once f_p had reached $2f_{PM}$ (=0.31 Hz), a sudden wind shift was introduced. Seven cases were investigated, corresponding to wind shifts of 0°, 30°, 60°, 90°, 120°, 150° and 180°.

4. Duration limited growth

Both numerical models have been tested and found to perform well under fetch limited conditions, for which there is an abundance of field data (Hasselmann et al., 1985). A similar evaluation for even the simplest of the current experiments, duration limited growth (zero wind shift), is virtually impossible because of lack of suitable field data. Some indication of model performance can, however, be obtained by a comparison with the two-parameter wave growth model of Hasselmann et al. (1976). For the case of duration limited growth for a constant wind field, this model yields the growth relationships (assuming $28u_* = U_{10}$)

$$f_p^* = 2.50(t_*)^{-3/7} \tag{4.1}$$

$$\alpha = 0.29(f_p^*)^{2/3} \tag{4.2}$$

$$\epsilon^* = 4.57 \times 10^{-5}(f_p^*)^{-10/3} \tag{4.3}$$

where $f_p^* = f_p u_*/g$, $t^* = tg/u_*$ and $\epsilon^* = \epsilon g^2/u_*^4$.

Figure 1 shows a comparison between the nondimensional JONSWAP parameters obtained from both models and Eqs. (4.1)–(4.3). The agreement is reasonable, particularly when it is remembered that Eqs. (4.1)–(4.3) represent solutions of parametric equations based on field data, for which there is significant scatter, and apply only for self-similar spectra, i.e., for the initial and main growth stages, but not in the transition region to a fully developed spectrum. For both models, the parameters ϵ, f_p^*, α and γ reproduce expected trends and asymptotically approach the Pierson–Moskowitz values at large values of t^*.

The best agreement between the models EXACT-NL and 3G-WAM is seen in the growth of the scale parameters, the peak frequency f_p^* and energy ϵ^*. The shape parameters α and γ show some deviations. This is because the parameterized model generates a somewhat broader spectrum around the peak, resulting in reduced α and γ values. The effect is seen more clearly in Fig. 2, where the one-dimensional spectra $F^*(f)$ are plotted against nondimensional time, t^*. Deviations of the model shape parameters are probably not too serious, as the shape parameters are much more poorly determined by data than the scale parameters. The

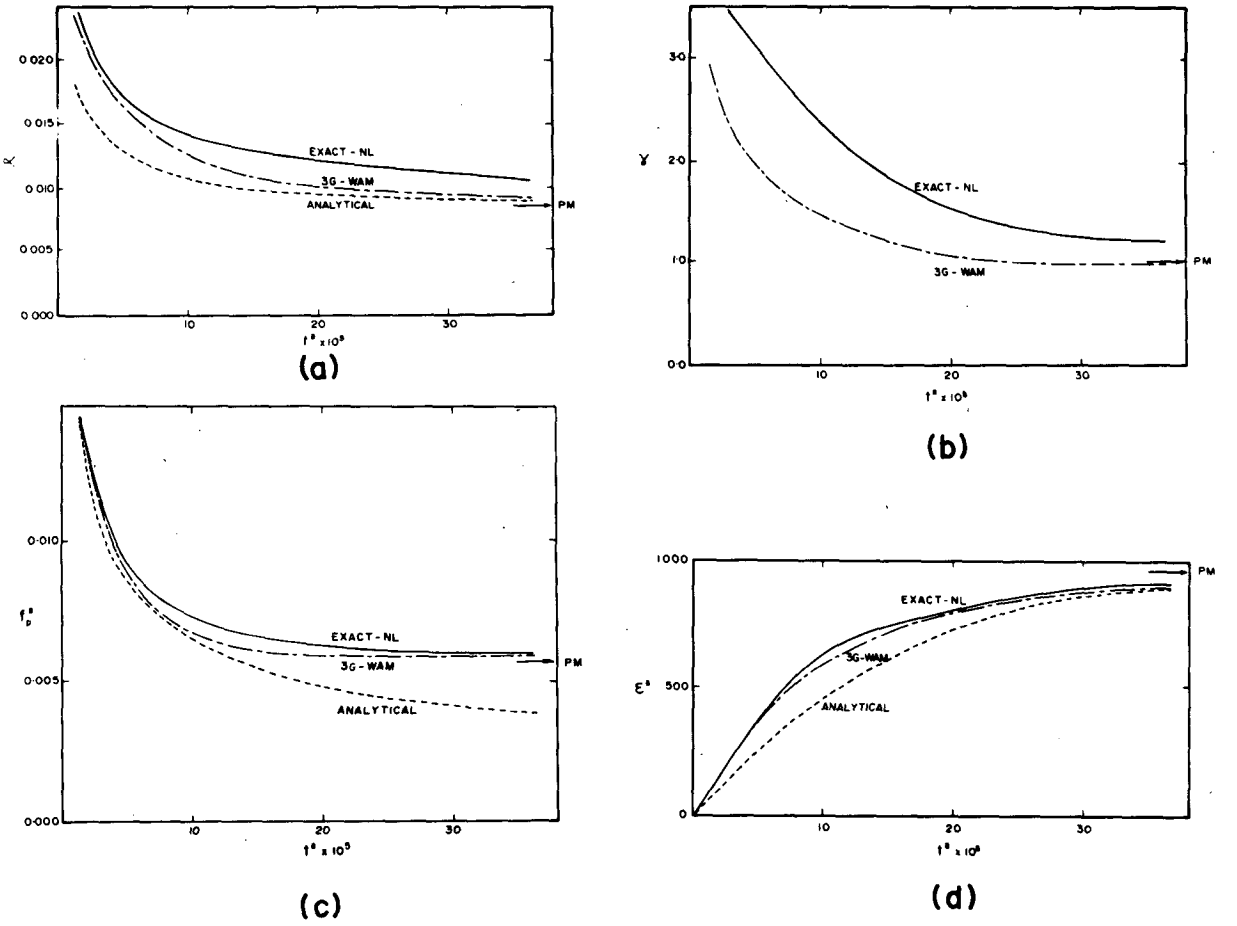

FIG. 1. Comparison between the nondimensional JONSWAP parameters obtained from EXACT-NL, 3G-WAM and the analytical solution of Eqs. (4.1)–(4.3) for the case of duration-limited growth.

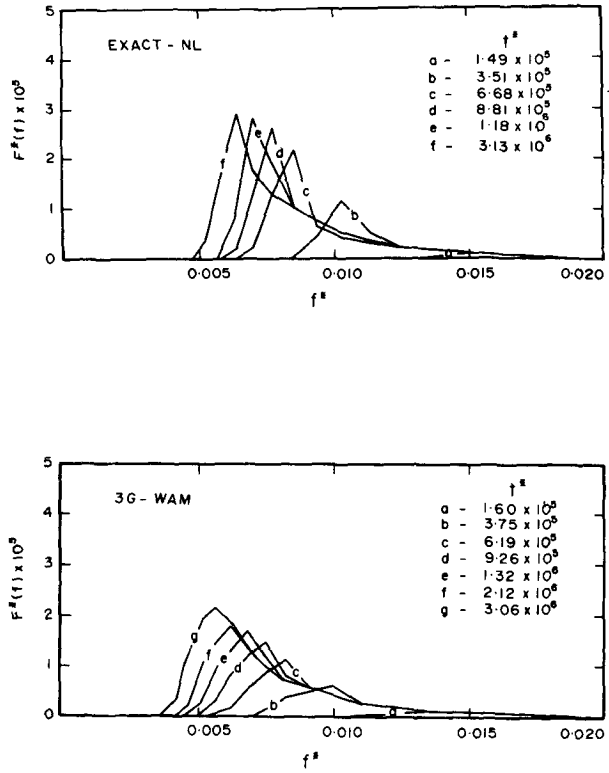

FIG. 2. Development of the one-dimensional spectrum $F^*(f)$ with nondimensional time for duration-limited growth.

JONSWAP shape parameters (Hasselmann et al., 1973), for example, show a scatter in α and γ that significantly exceeds the differences in Figs. 1a, b between EXACT-NL and 3G-WAM.

Figure 3 shows the growth of four individual spectral components as a function of t^*. Both models clearly reproduce the "overshoot effect," as first reported by Barnett and Wilkerson (1967). The relative magnitude of the overshoot is larger for the full model, particularly at lower frequencies. The model also exhibits an undershoot for higher frequencies, as observed similarly in fetch-limited wave growth experiments (cf. Mitsuyasu, 1968a, b, 1969).

The individual source terms S_{in}, S_{dis} and S_{nl} are shown together with the net source function S_{tot} in Fig. 4 for the early and asymptotic growth stages. The energy balance is qualitatively similar for both models, although difference exists in detail due to the slightly different spectral shapes produced by the two models (cf. also Hasselmann et al., 1985). The over- and undershoot effect is clearly seen to result from the nonlinear transfer, as originally surmized by Barnett and Sutherland (1968) and later confirmed by more extensive experiments and computations (e.g., Mitsuyasu, 1968a, b; Hasselmann et al., 1974).

At frequencies significantly greater than the spectral peak, an approximate balance exists between the three source terms, $S_{tot} \approx 0$. This balance is responsible for the fetch or duration independent shape of the high-frequency portion of the spectrum. Examination of the details of the spectral evolution in the present experiments, and in the more extensive set of wave–wave interaction calculations by Komen et al. (1984) and Young et al. (1985), indicates that the nonlinear term plays a key role in this shape-stabilizing process. Whenever a small peak or trough develops in the high-frequency portion of the spectrum as the result of a local source term imbalance, the nonlinear interactions quickly remove the anomaly by redistributing the energy over neighboring frequency bands, thereby restoring the spectrum to a stable quasi-equilibrium shape. This effect becomes particularly marked in the turning-wind situations. The equilibrium shape is found to lie fairly close to the f^{-4} form proposed by Zakharov and Filonenko (1966), Zakharov and Zaslavskii (1982) and Kitaigorodskii (1983). However, the basic assumption of these authors of a divergence-free nonlinear energy cascade down the spectrum is found to be inconsistent with the observed rate of growth of a wind-sea spectrum (cf. Komen et al., 1984). Alternative dimensional arguments for an f^{-4} spectrum have been put forward by Toba (1973) and others.

In the earlier stages of growth (Figs. 4a and 4c), the peaked spectral shape, reflected by the high values of γ in Fig. 1b, caused a pronounced plus–minus signature in S_{nl}, and consequently in S_{tot}. The positive lobe of the transfer occurs slightly to the left of the spectral peak and, as already discussed in Hasselmann et al. (1973), is responsible for the migration of the spectral peak to lower frequencies. The negative lobe to the right of the spectral peak results in a gradual broadening of the spectrum, as well as in a rapid reduction of energy during the undershoot following the overshoot in Fig. 3. The relative magnitude of the negative lobe is greater in the model EXACT-NL, resulting in a more pronounced overshoot/undershoot signal and a more strongly peaked spectrum.

As the spectrum approaches full development (Figs. 4b and 4d), the source term balance changes significantly. The broader and less peaked shape of the spectrum results in a reduction of the nonlinear transfer by almost an order of magnitude. The positive lobe now lies under the peak and is balanced by the dissipation, while the much broader negative lobe balances the atmospheric input. The result is an almost complete balance of the source terms across the entire spectrum, as required, of course, for a fully developed equilibrium state. This regime is essentially identical to the fully developed state discussed in the fetch-limited growth studies of Komen et al. (1984). (The last panel of Fig. 4d indicates some residual noise fluctuations of the net source function S_{tot}. This is typical for the instantaneous energy balance. Averaging over successive time steps reduces $\bar{S}_{tot}$ by an order of magnitude; cf. Komen et al., 1984).

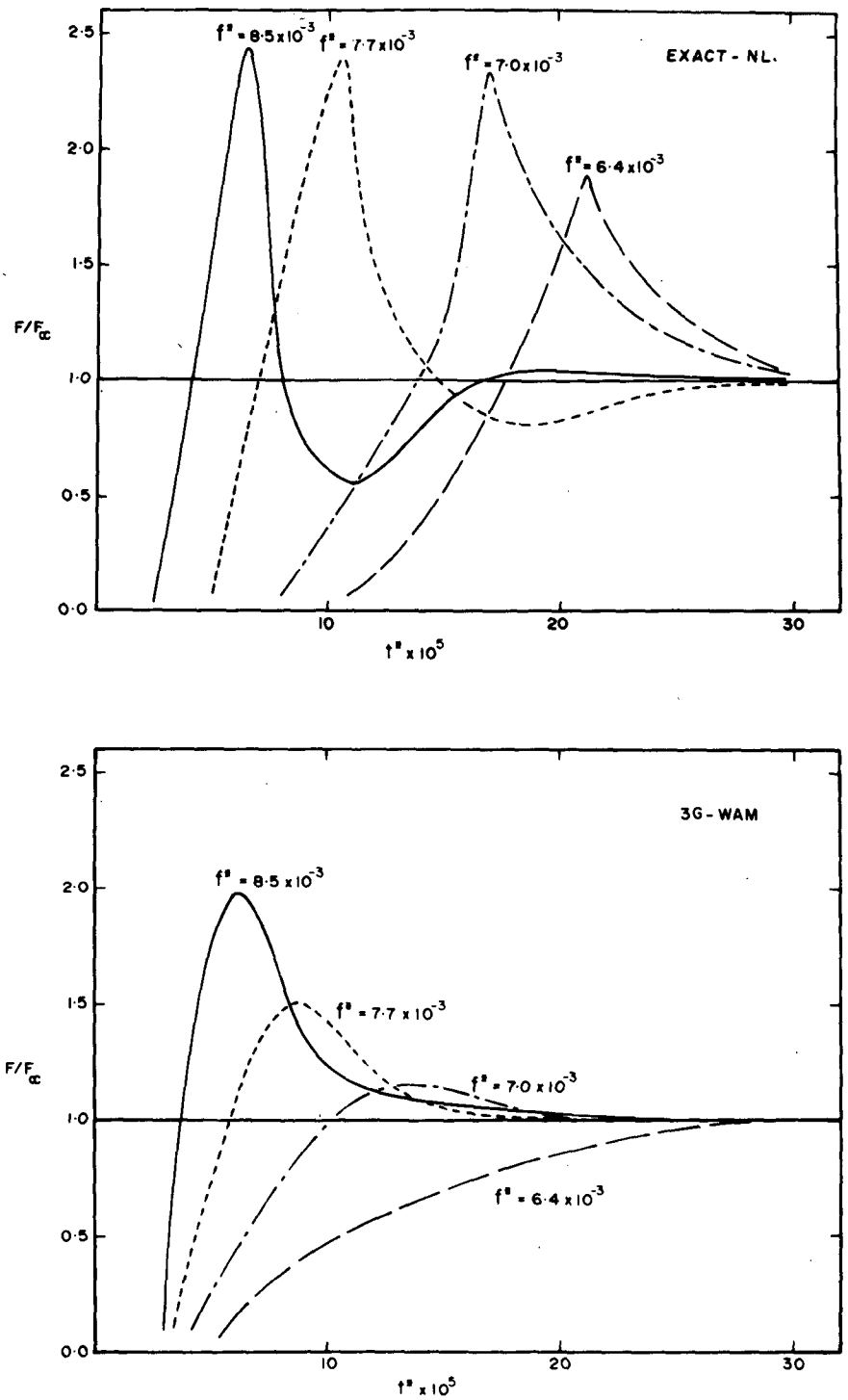

FIG. 3. Growth of individual spectral components with nondimensional time under duration-limited conditions. The "overshoot" effect observed under fetch-limited conditions is reproduced by both models.

5. Spectral evolution following a sudden wind shift

Contour plots of the two-dimensional wave spectra resulting from wind shifts of 30°, 60°, 90° and 120° are shown in Fig. 5 for both models. For each wind shift angle, the spectral evolution is shown as a function of the nondimensional time, measured from the point when the wind shift occurred (i.e., $\Delta t^* = t^* - t_0^*$,

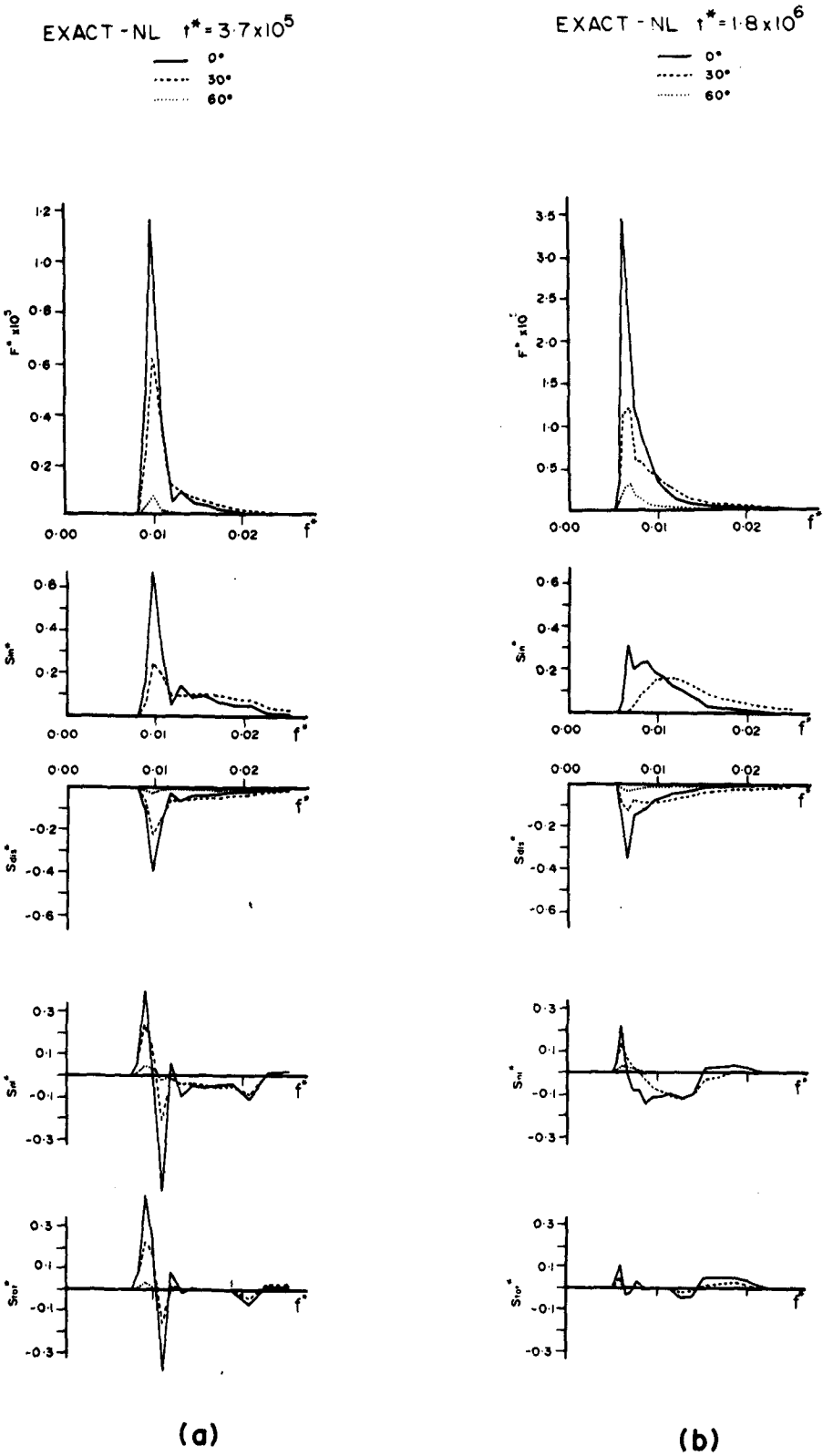

FIG. 4a–b. The source term balance for duration limited growth for the model EXACT-NL: (a) the early stages of growth, $t^* = 3.73 \times 10^5$, and (b) the asymptotic stage, $t^* = 1.79 \times 10^6$.

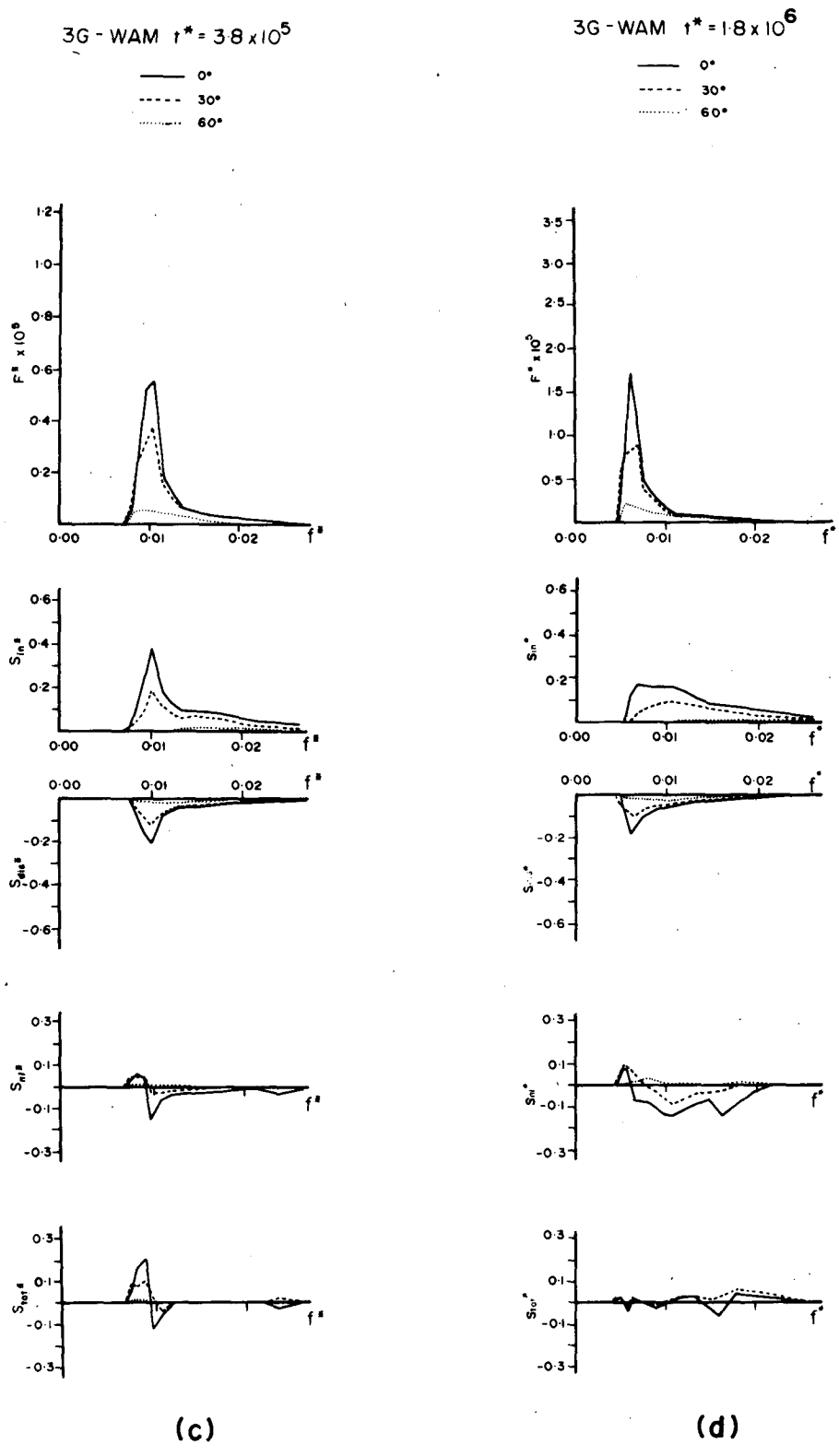

FIG. 4c–d. The source term balance for duration-limited growth for the model 3G-WAM: (c) the early stages of growth, $t^* = 3.75 \times 10^5$, and (d) the asymptotic stage, $t^* = 1.80 \times 10^6$.

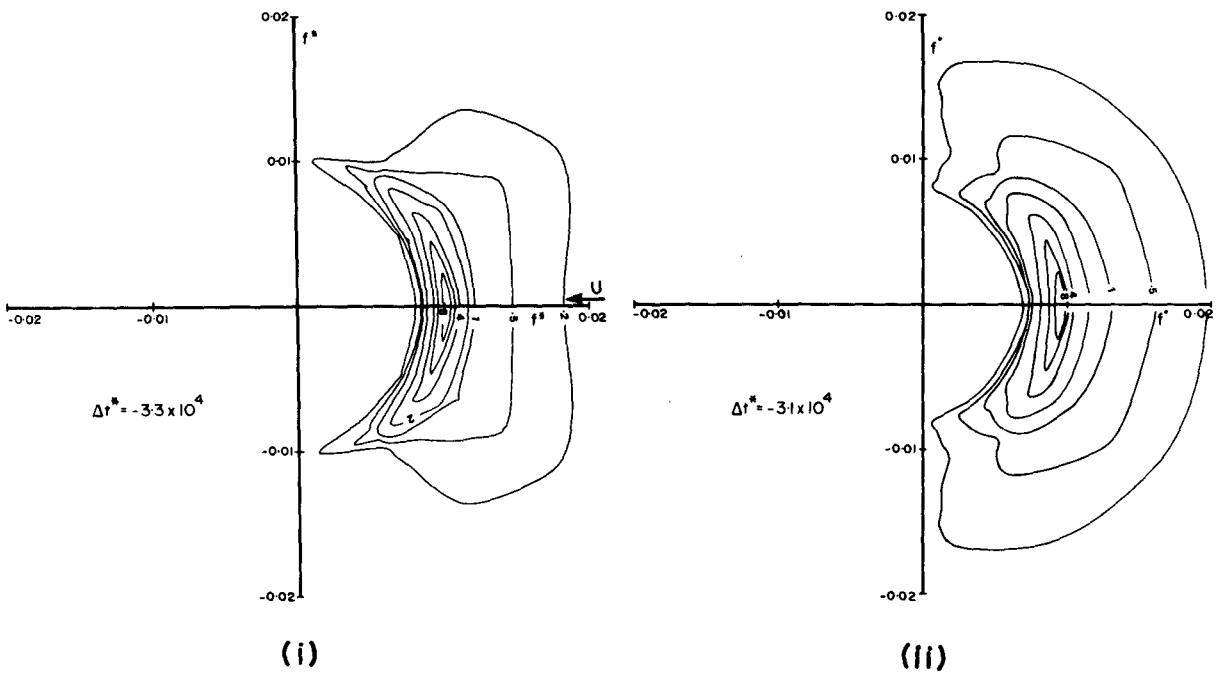

FIG. 5a. The directional wave spectra at $\Delta t^* \approx 0$, immediately prior to the wind shift. The spectra have been normalized such that the peak value is 10. The wind direction is shown by the arrow. (i) EXACT-NL, (ii) 3G-WAM.

$t_0^* = 4.1 \times 10^5$). At $\Delta t^* \approx 0$ (Fig. 5a) the model 3G-WAM shows a somewhat broader angular spread than the model EXACT-NL, in accordance with the broader peak of the 3G-WAM spectrum already discussed in the context of the one-dimensional frequency spectra.

The results of both models are quite similar for all wind shift cases. In both models there is a marked difference in the directional response for small and large wind shift angles. For wind shifts of 30° and 60°, the entire wind-sea spectrum rotates to the new wind direction, while for wind shifts of 90° or greater, a secondary wind sea, with a new high-frequency peak, is generated in the new wind direction.

The results for the small wind shift angles are in qualitative agreement with existing analyses of field measurements by Hasselmann et al. (1980), Günther et al. (1981) and Allender et al. (1983). The high-frequency components align more quickly with the wind than the low-frequency components. The frequency dependence of the directional relaxation results in a skewed spectral shape during the realignment process. After the entire spectrum is aligned in the new wind direction, further spectral growth continues in the normal manner for a duration limited sea. The time required for full alignment is almost identical in both models, namely, $\Delta t^* \approx 5 \times 10^5$ for $\Delta\phi = 30°$ and $\Delta t^* \approx 6 \times 10^5$ for $\Delta\phi = 60°$. The behavior of the spectral peak, however, is slightly different in the two models. In the parameterized model, the frequency of the spectral peak remains almost constant during the realignment process, while in the model EXACT-NL a gradual shift of the spectral peak occurs to lower frequencies.

The processes governing the realignment of the spectra can be understood by examining the source term balances shortly after the wind shift has occurred (Fig. 6). For both shift cases, $\Delta\phi = 30°$ and 60° (Figs. 6a and 6b), an almost perfect balance (i.e., $S_{tot} = 0$)

TABLE 1. Values of the relaxation coefficient, b, determined for the model EXACT-NL.

f (Hz)	U_{10}/c	b ($\tilde{\theta} = 30°$)	b ($\tilde{\theta} = 60°$)
0.25	1.60	4.3×10^{-5}	4.2×10^{-5}
0.34	2.18	1.1×10^{-4}	1.0×10^{-4}
0.40	2.56	1.6×10^{-4}	1.5×10^{-4}
Average		$\sim 1.0 \times 10^{-4}$	$\sim 1.0 \times 10^{-4}$

TABLE 2. Values of the relaxation coefficient, b, determined for the model 3G-WAM.

f (Hz)	U_{10}/c	b ($\tilde{\theta} = 30°$)	b ($\tilde{\theta} = 60°$)
0.25	1.60	4.5×10^{-5}	4.5×10^{-5}
0.34	2.18	1.4×10^{-4}	1.4×10^{-4}
0.40	2.56	2.0×10^{-4}	2.0×10^{-4}
Average		$\sim 1.3 \times 10^{-4}$	$\sim 1.3 \times 10^{-4}$

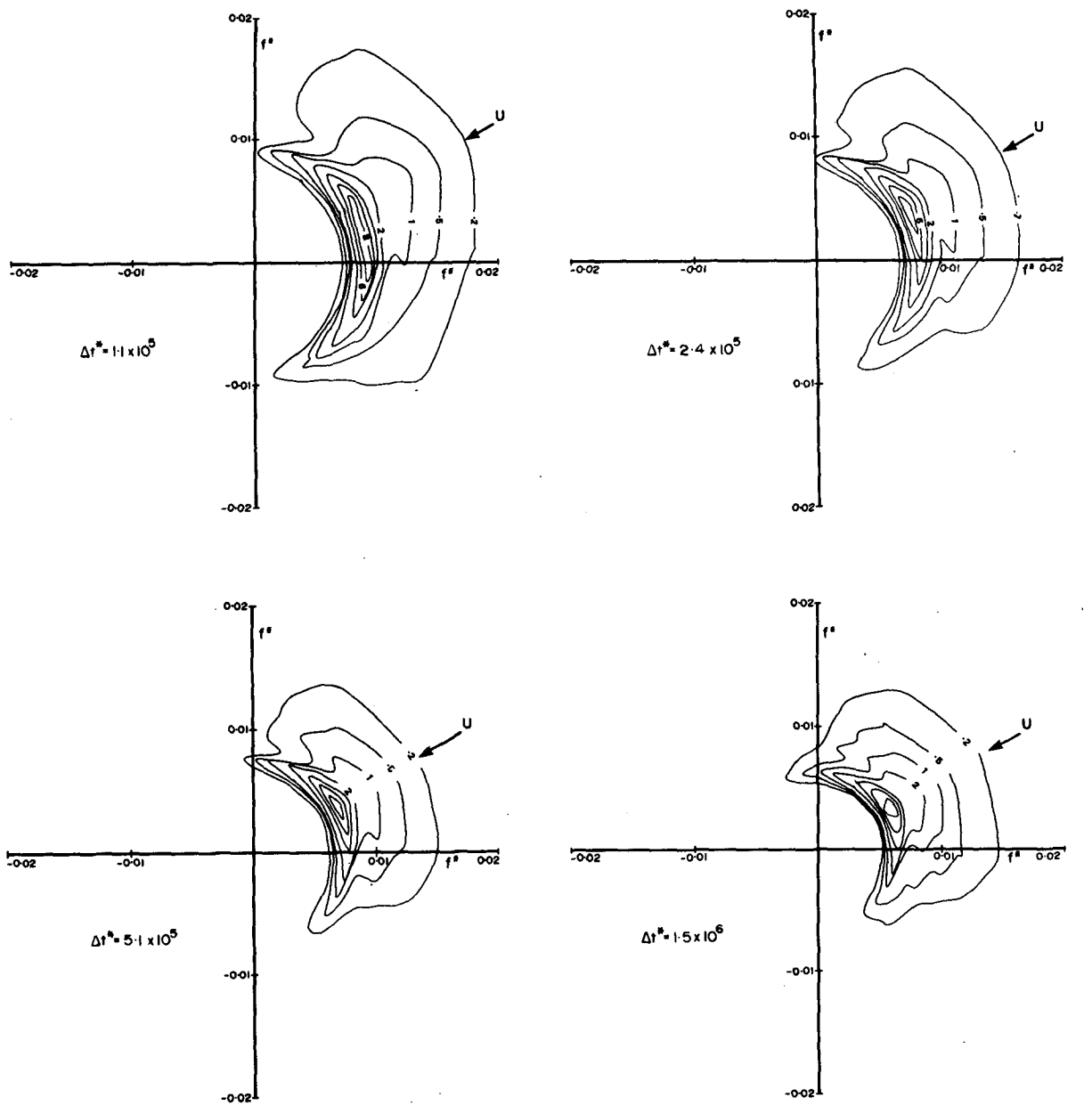

FIG. 5b. (i) Evolution of the directional wave spectrum with time for a wind shift of 30° from model EXACT-NL.

exists at high frequencies. This indicates that the high frequency components respond almost immediately to the wind shift and are now in equilibrium with the new wind direction. The source function S_{in} has a bimodal frequency distribution, the higher frequency peak being aligned with the new wind direction, as expected. This input would tend to cause a new high-frequency peak to develop in the spectrum. However, this is counteracted by the nonlinear wave–wave interactions. In addition to the normal positive/negative lobe structure, S_{nl} develops a second broader negative region that almost exactly mirrors the high-frequency peak in the S_{in} term. Thus the nonlinear interactions prevent the growth of a secondary peak within the spectrum by coupling the peak to the already existing more stable unimodal structure. Both the present results and the more extensive calculations of Young et al. (1985) indicate that, even when such secondary peaks are separated by as much as 60° from the dominant wave direction, the nonlinear coupling to the dominant wave components is still sufficiently strong to prevent the secondary peak from growing.

At lower frequencies, the shape of the S_{nl} term is qualitatively similar to the normal duration-limited

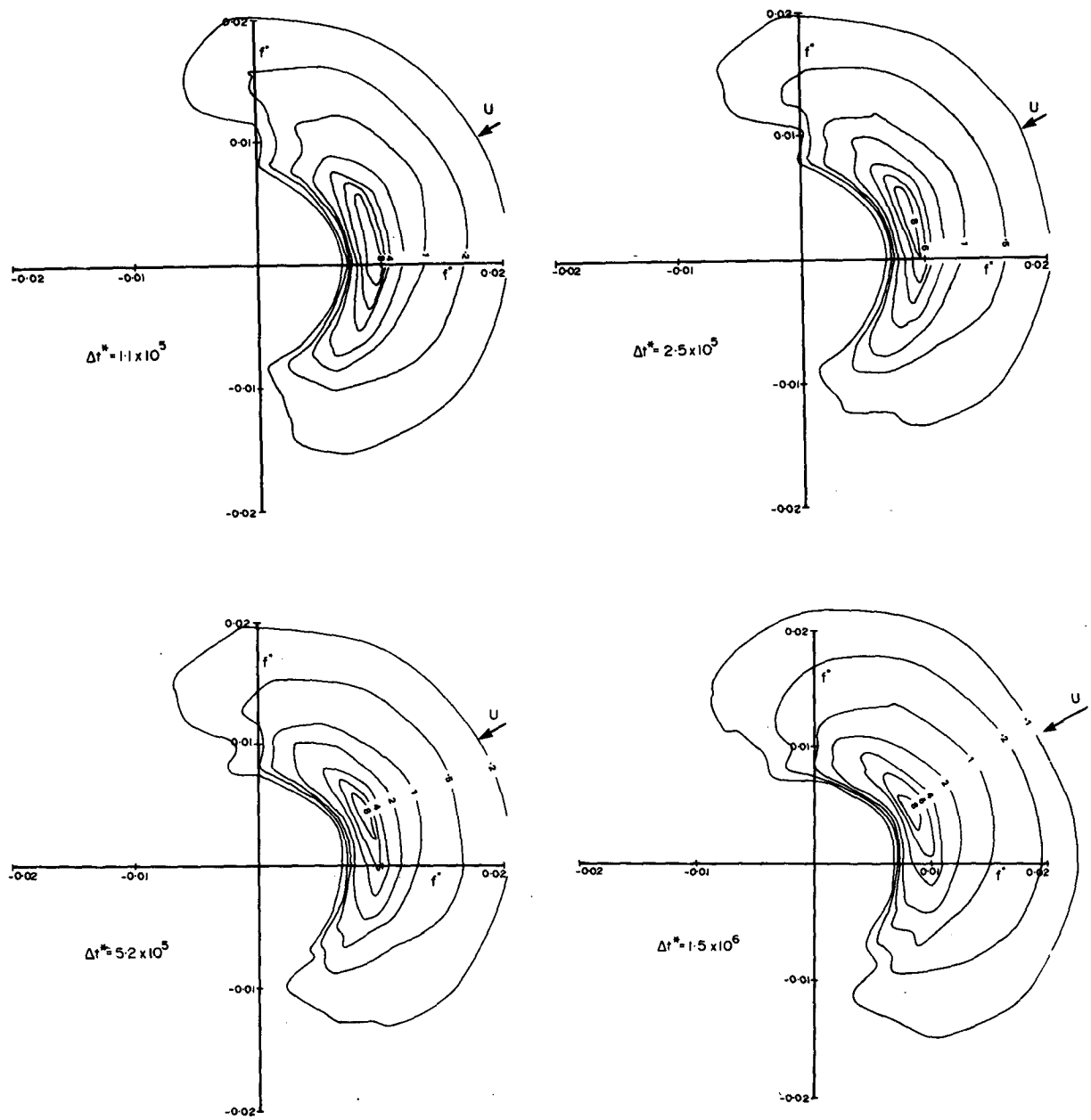

FIG. 5b. (ii) As in Fig. 5b(i) but for the model 3G-WAM.

growth situation. The gradual directional relaxation of the spectrum in this frequency range is brought about by the imbalance between the S_{in} and S_{dis} terms. In the old wind direction, the atmospheric input is reduced through the cosine term in Eq. (2.2), whereas the dissipation, which is proportional to the local energy spectrum with a directionally independent proportionality factor, is still a maximum. The imbalance results in a gradual decay of energy in the old wind direction. In the new wind direction, on the other hand, the role of these terms is reversed, resulting in a net growth. The combination of gradual growth of energy in the new wind direction and decay in the old direction results in a smooth rotation of the mean wave spectrum direction. The nonlinear coupling between components near the spectral peak is stronger in the model EXACT-NL than in the parameterized model 3G-WAM. This results in an enhanced positive lobe in the nonlinear transfer and explains the continual migration of the spectral peak to lower frequencies during the realignment process in this model (Figs. 5b and 5c).

For a wind shift of 90°, the spectral response changes markedly (Fig. 5d). Both models indicate that, initially, a high-frequency peak begins to develop at approxi-

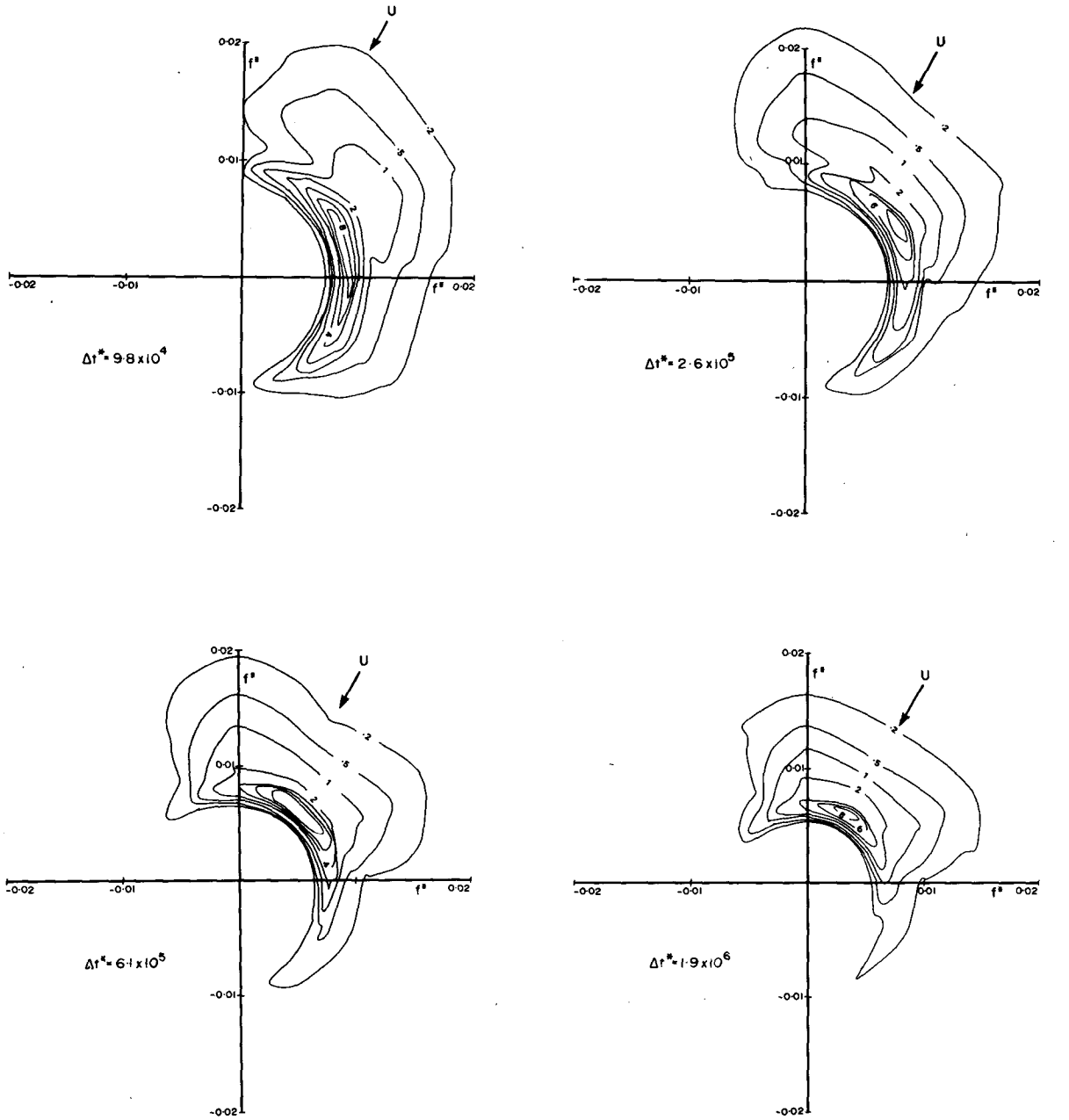

FIG. 5c. (i) Evolution of the directional wave spectrum with time for a wind shift of 60° from model EXACT-NL.

mately 70°. The 20° offset relative to the wind direction is due to the fact that the S_{in} term is proportional to the spectrum and thus requires some initial level of energy to become effective. The product of the wind input proportionality factor and the initial spectral spreading function oriented about the old wind direction peaks near 70°. As growth continues, the peak quickly rotates to 90°. Once aligned in the new wind direction, the new wind sea grows almost independently of the old sea, which gradually decays under the action of the S_{dis} term.

Examination of the source term balance shortly after the wind shift (Fig. 6c) confirms the skewing of the atmospheric input toward the old wind direction. For the full model, the two seas at 0° and 90° are now sufficiently separated in directional space that the nonlinear coupling between them becomes almost negligible, the S_{nl} distribution being composed simply of the superposition of the contributions for the two seas. The nonlinear transfer at 90° is significantly greater than at 0° because of the more highly peaked form of the new wind-sea spectrum. Although the coupling be-

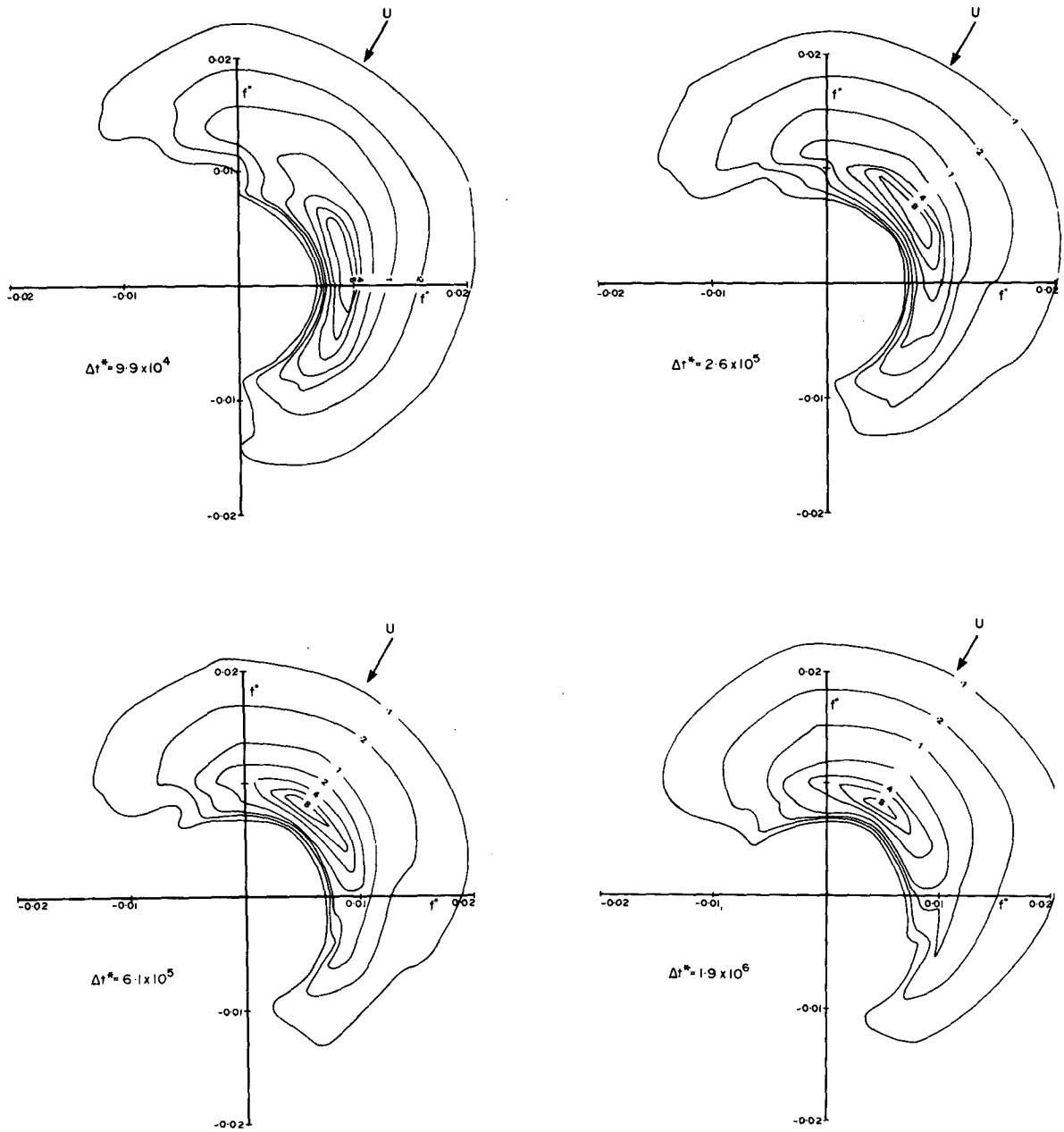

FIG. 5c. (ii) As in Fig. 5c(i) but for the model 3G-WAM.

tween the separate seas is stronger in the parameterized model, the development of the spectrum is still very similar to the full model. In both cases the net source term, S_{tot}, shows a decay of the old sea, due mainly to the imbalance $S_{in} < S_{dis}$, while the wind sea at 90° exhibits a growth very similar to the standard duration-limited situation.

For a wind shift of 120°, the response is very similar to that at 90°. Initial growth occurs at approximately 90° due to the product nature of the S_{in} term and the initial directional spread of the old wind sea. The new wind sea, however, quickly aligns with the new wind direction, and the two seas then become dynamically decoupled (except for the common integral slope factor in the dissipation expressions). The wave field thus reduces to the superposition of a duration limited wind sea and a decaying swell. Both models produce almost identical results.

Cases with wind shifts of 150° and 180° were also investigated. As expected, the adjustment processes

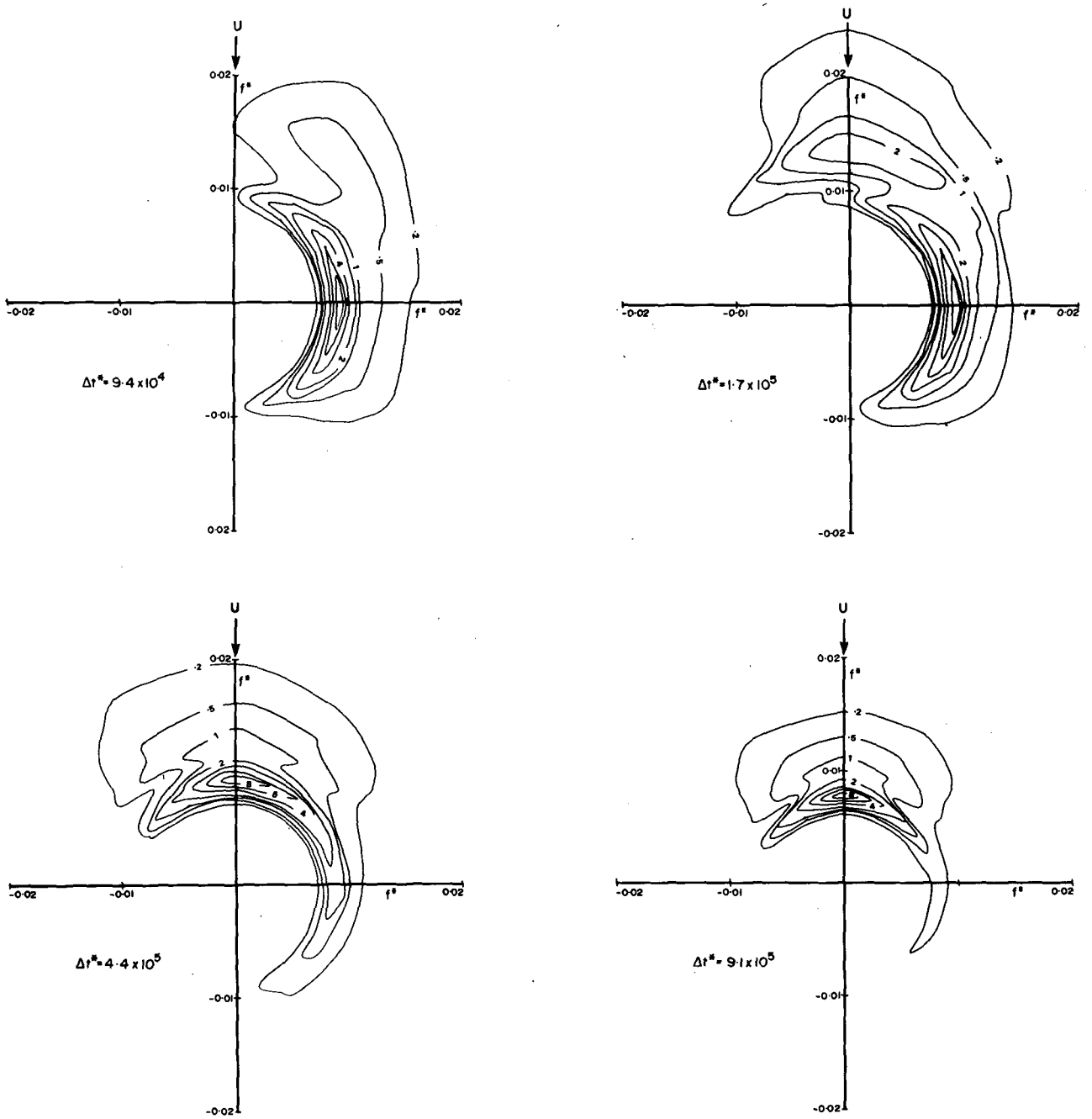

FIG. 5d. (i) Evolution of the directional wave spectrum with time for a wind shift of 90° from model EXACT-NL.

were very similar to the 120° case, the wave field again adjusting very rapidly to a superposition of a decoupled wind sea and a swell system.

6. Comparison with field data

Comparison of the present results with field data is difficult due to the paucity of relevant data and the unavoidable contaminations of temporal wind field changes by spatial inhomogeneities. To date, only two datasets have been published: the JONSWAP 1973 data (Hasselmann et al., 1980, Günther et al., 1981) and the data of Allender et al. (1983). Both datasets yielded similar results. The directional relaxation could be represented by relations of the form

$$\frac{d\theta}{dt} = \omega b \sin(\theta_w - \theta) \tag{6.1}$$

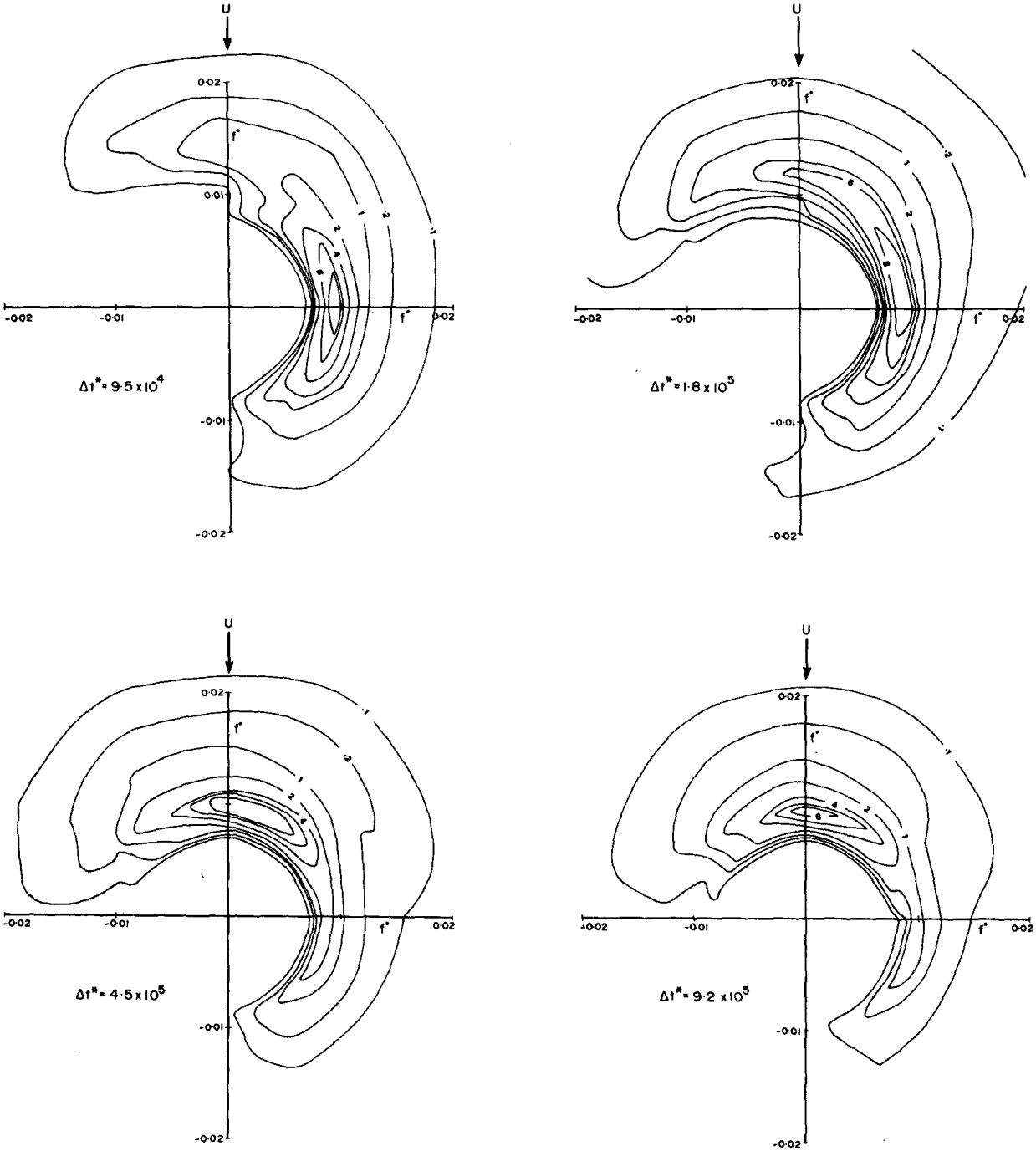

FIG. 5d. (ii) As in Fig. 5d(i) but for the model 3G-WAM.

where $b \approx 3 \times 10^{-5}$, $\theta_w(t)$ is the wind direction, and $\theta(t)$ is the mean wave direction. For a step change in wind direction from $\theta_w = 0$ to $\theta_w = \tilde{\theta}$, integration of Eq. (6.1) yields

$$\omega bt = -\ln \frac{\tan[(\tilde{\theta} - \theta)/2]}{\tan(\tilde{\theta}/2)}. \tag{6.2}$$

Our computations indicate that a continuous angular relaxation relation, as assumed in this analysis, is valid only for wind shift values $\tilde{\theta}$ of 60° or less. However, this condition was satisfied for both datasets.

To estimate the relaxation coefficient b appropriate for our computations, Eq. (6.2) was fitted to the computed response for $\tilde{\theta} = 30°$ by a regression analysis (Tables 1 and 2).

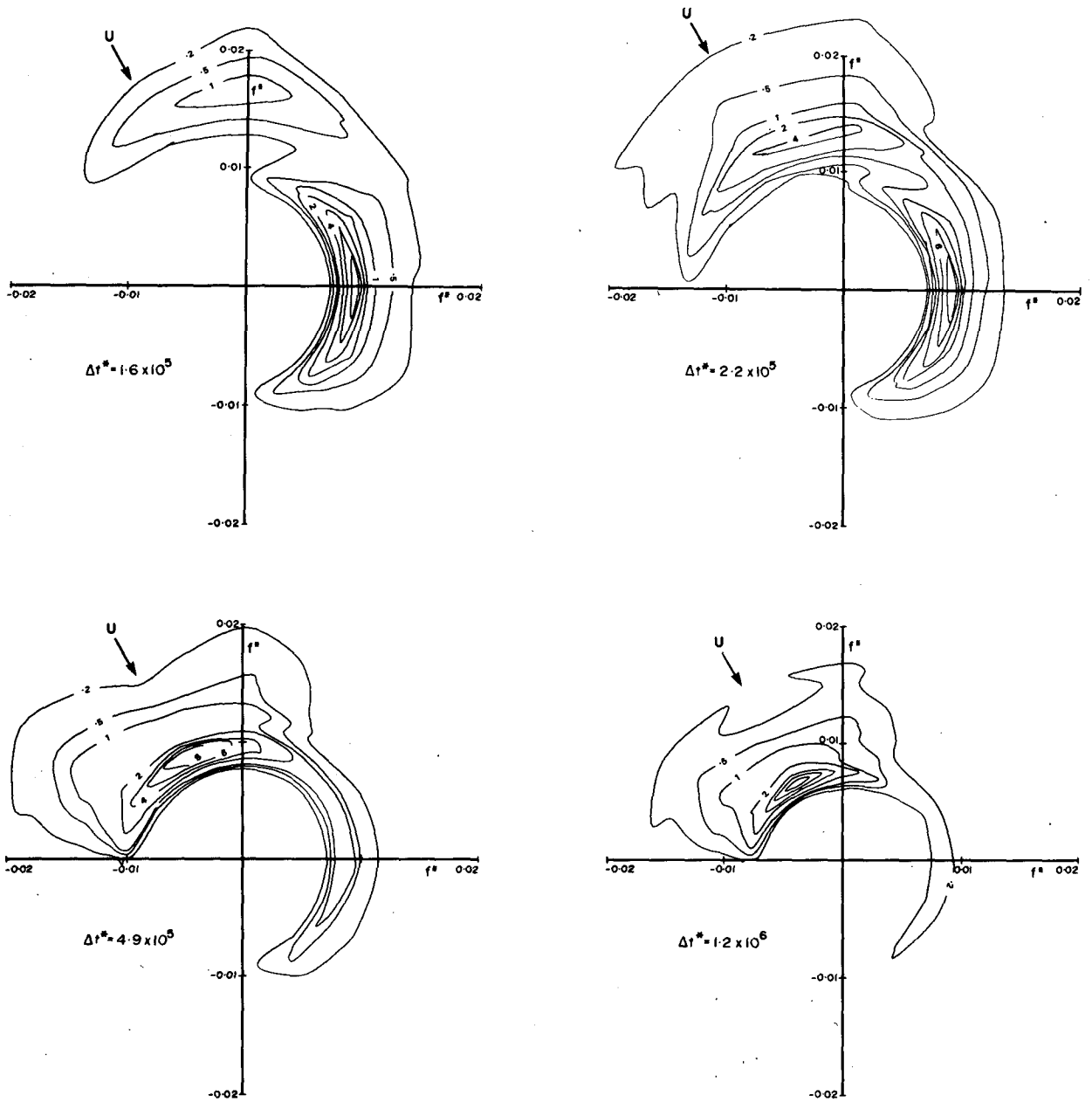

FIG. 5e. (i) Evolution of the directional wave spectrum with time for a wind shift of 120° from model EXACT-NL.

Both models yield similar average relaxation coefficients of approximately 1×10^{-4}. This value is significantly larger than the value 3×10^{-5} obtained from field data. However, as can be seen from Tables 1 and 2, b is not constant, but varies with U_{10}/c. As is to be expected, the "younger," high-frequency components tend to align with the wind more rapidly than the "older," low-frequency components. Hence a comparison between the present results and field data is valid only at comparable values of U_{10}/c. The data of both Hasselmann et al. (1980) and Allender et al. (1983) corresponded to U_{10}/c values lying between 1.0 and 1.8. For this parameter range, the numerical models yield a value of $b \approx 4 \times 10^{-5}$, in reasonable agreement with the measured value of 3×10^{-5}.

The potential importance of U_{10}/c was recognized by Hasselmann et al. (1980), but the scatter in their data prevented a determination of the variation of b as a function of this variable. In the present models, the rate of directional relaxation is determined by the rather subtle balance between the atmospheric input, dissipation and nonlinear coupling as discussed in section 5, so that a dependence on u_*/c (or U_{10}/c) must be expected through the dependence of the atmospheric

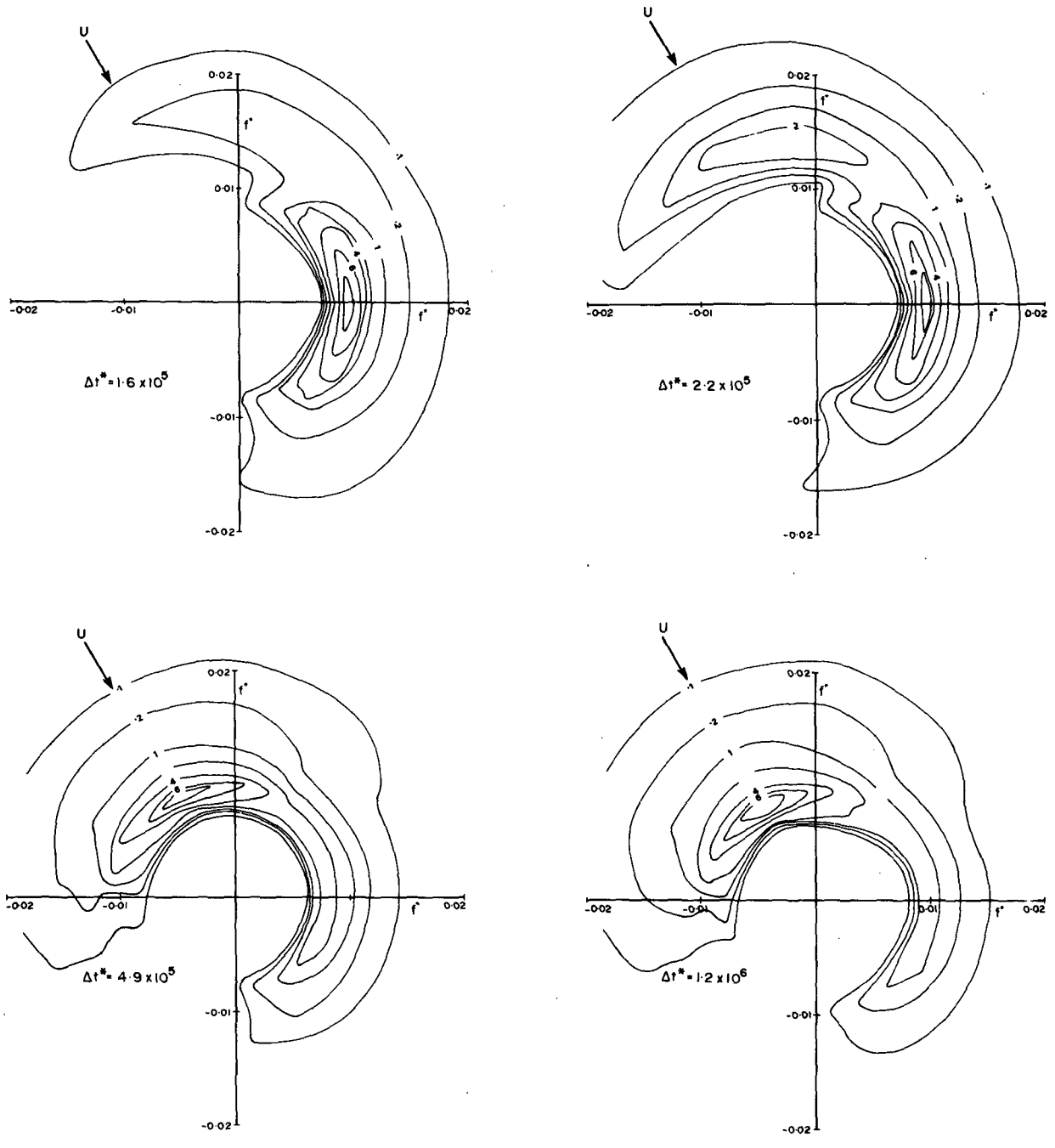

FIG. 5e. (ii) As in Fig. 5e(i) but for the model 3G-WAM.

input on this parameter. Furthermore, because of its influence on the nonlinear transfer, the "wave age" parameter $u_*/c_p = u_*\omega_p/g$ (which was held constant in the present experiments) will, in general, also affect the directional relaxation process. Since two parameters alone are needed to characterize the simple case of a step function change in direction of a homogeneous wind field—which itself already represents a strongly idealized special situation—we have not attempted to summarize our results in a general formula. The purpose of our experiment was rather to clarify the interplay of the various mechanisms that control the directional response of the wave field in complex wind situations and to demonstrate the feasibility of simulating these processes with realistic numerical wave models.

7. Conclusion

An extensive set of numerical experiments has been performed with two numerical wave models, EXACT-

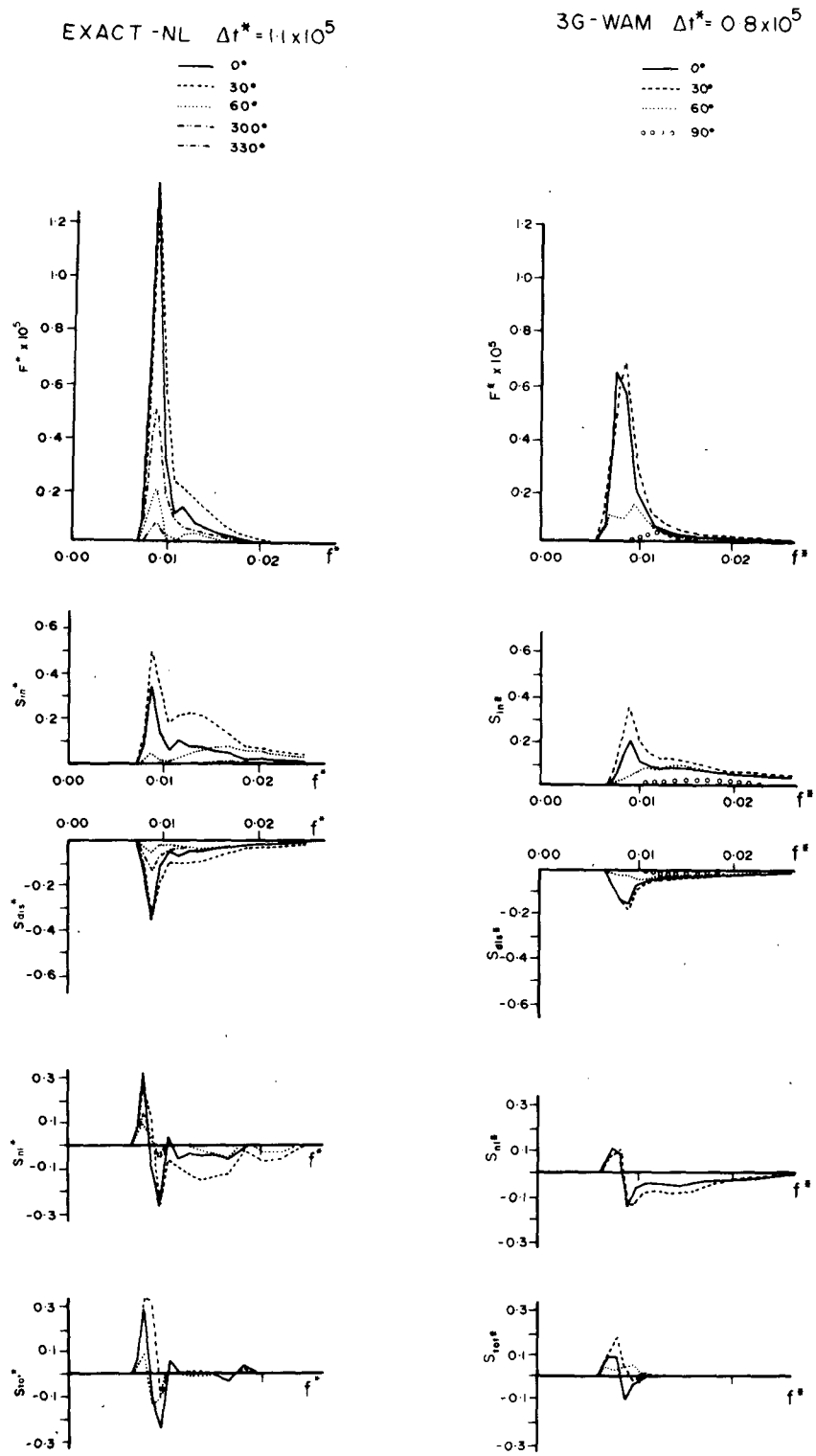

FIG. 6a. The source term balance shortly after a wind shift of 30°, $\Delta t^* \approx 1.1 \times 10^5$.

NL and 3G-WAM, to determine the processes controlling the directional response of ocean waves for a sudden change in wind direction. In contrast to existing second generation models, both models introduce no a priori assumptions regarding the shape of the spectrum.

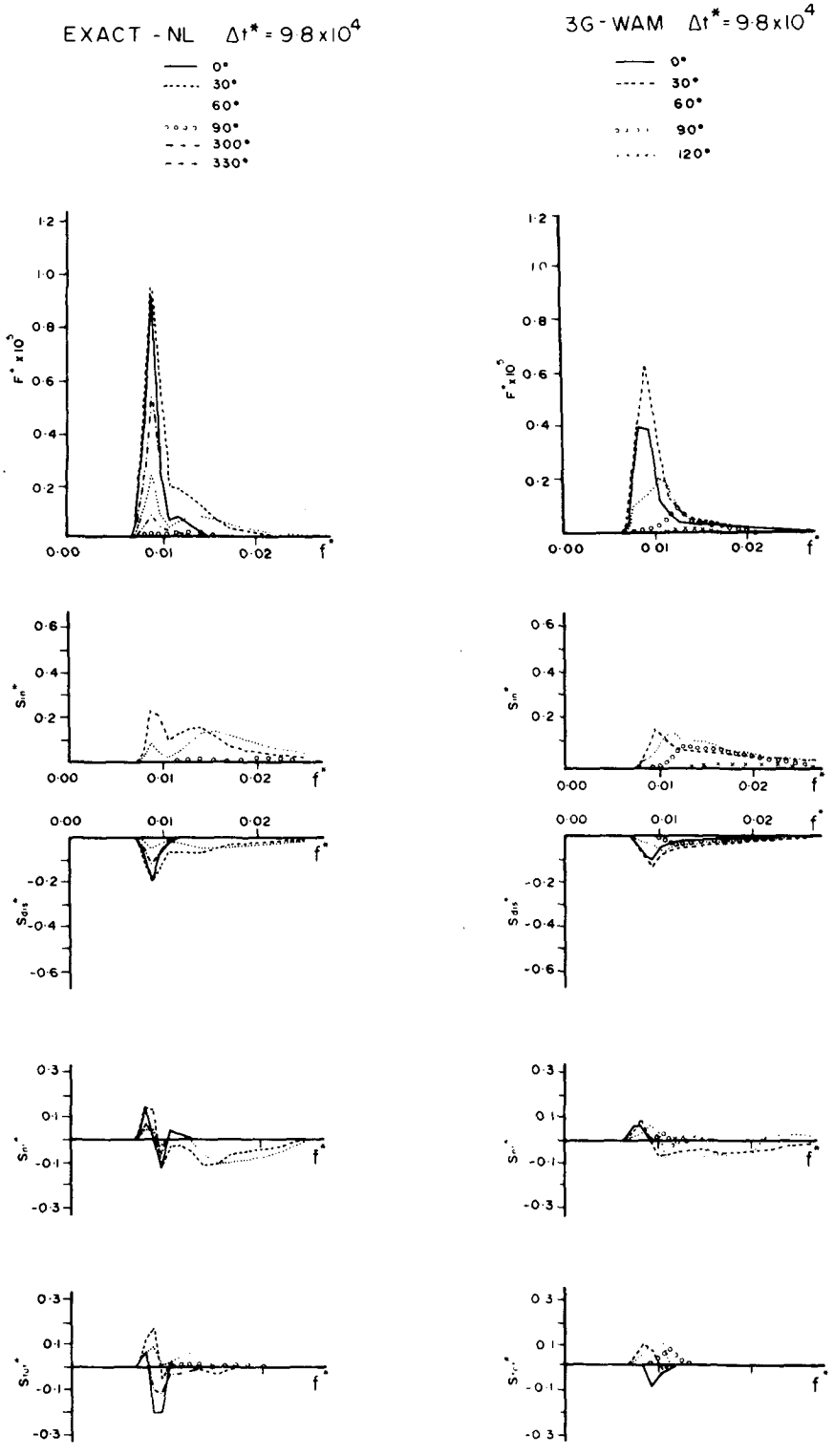

FIG. 6b. As in Fig. 6a but for a wind shift of 60°, $\Delta t^* \approx 1.0 \times 10^5$.

For wind shifts of 60° or less, the entire spectrum rotates into the new wind direction. The (dimensionless) relaxation rate is a function of u_*/c (among other spectral parameters), the alignment with the new wind direction occurring faster for high-frequency components than for low frequencies. The tendency for a sec-

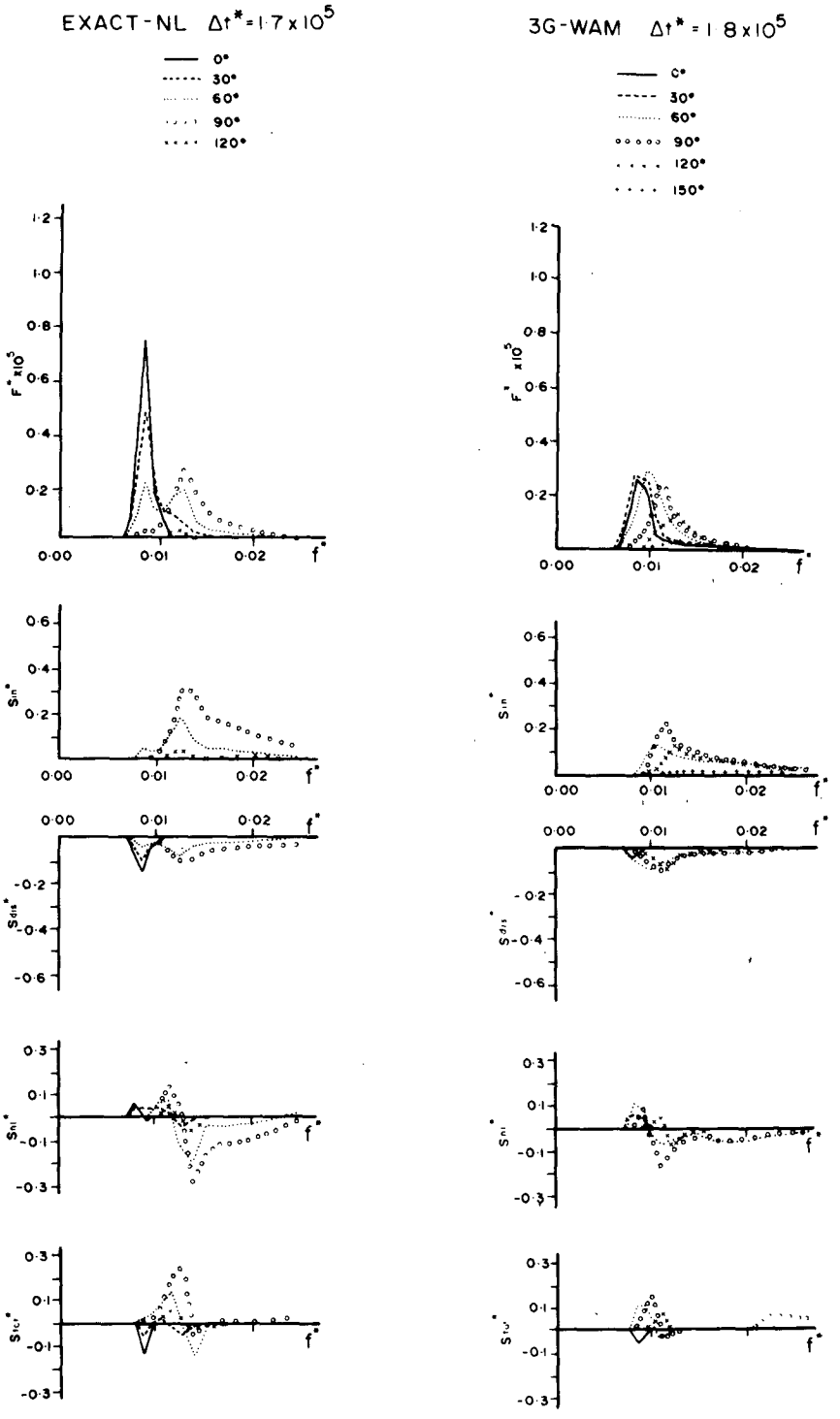

FIG. 6c. As in Fig. 6a but for a wind shift of 90°, $\Delta t^* \approx 1.7 \times 10^5$.

ondary spectral peak to develop in the new wind direction is suppressed for these wind shift angles by the stabilizing influence of the nonlinear wave–wave interactions, which tend to favor a unimodal spectral distribution.

At angles of 90° and greater the coupling between the old sea and the newly generated wind waves becomes sufficiently weak that the wave–wave interactions are unable to suppress the development of a new high-frequency wind-sea peak in the new wind direc-

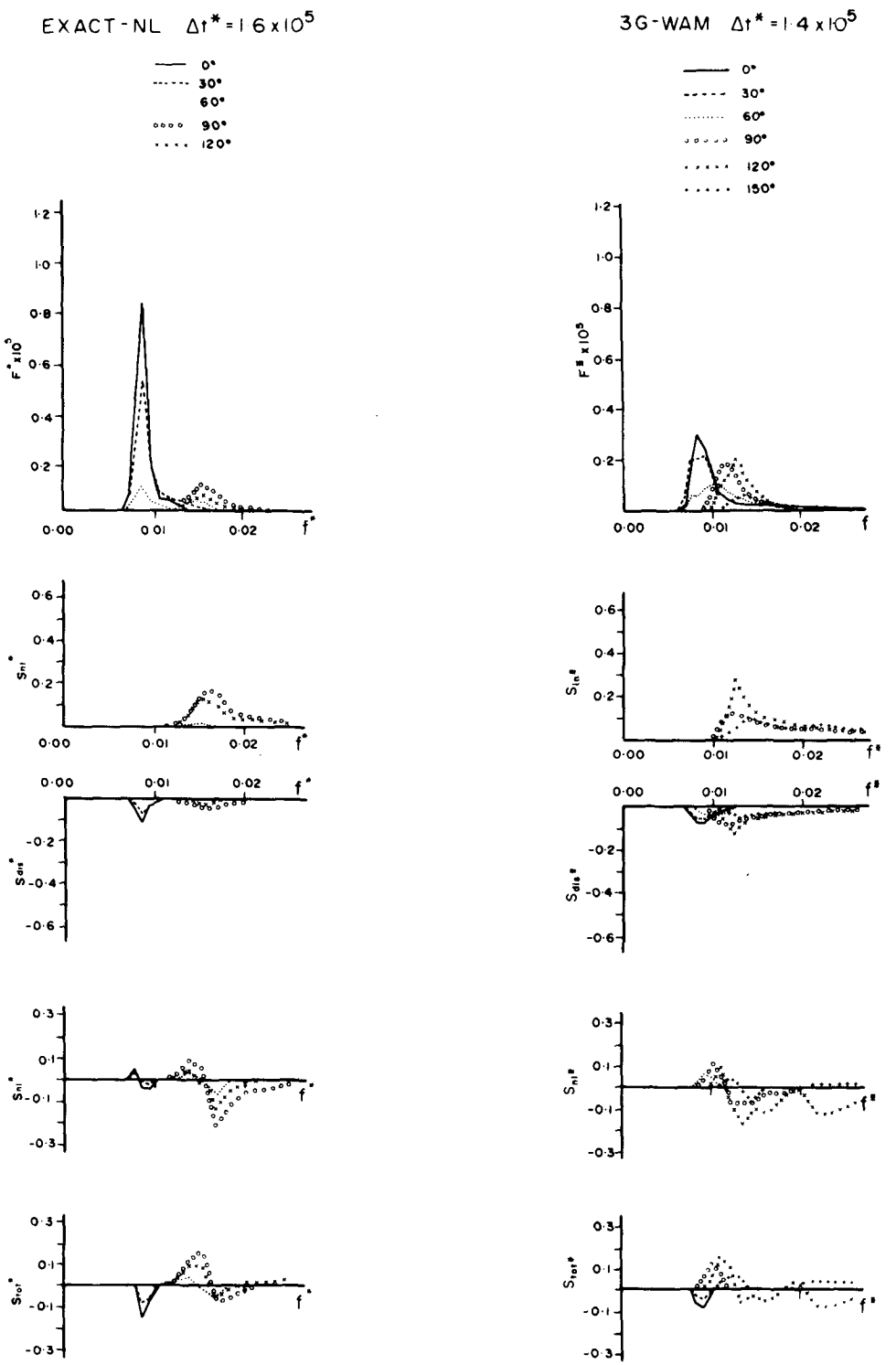

FIG. 6d. As in Fig. 6a but for a wind shift of 120°, $\Delta t^* \approx 1.5 \times 10^5$.

tion. The new wind sea develops independently of the old sea, which is gradually transformed into quasi-linear swell and decays under the action of the dissipation term.

The important role of the nonlinear interactions in these experiments underlines the need for an accurate approximation for this source term in spectral wave models. In particular, operator parameterizations of

S_{nl} are required which (as in 3G-WAM) are applicable to an arbitrary spectrum and retain the general stabilizing, redistributive features of the exact transfer expression.

REFERENCES

Allender, J. H., J. Albrecht and G. Hamilton, 1983: Observations of directional relaxation of wind sea spectra. *J. Phys. Oceanogr.*, **13,** 1519–1525.

Barnett, T. P., and J. C. Wilkerson, 1967: On the generation of ocean wind waves as inferred by airborne radar measurements of fetch-limited spectra. *J. Mar. Res.*, **25,** 292–328.

——, and A. J. Sutherland, 1968: A note on an overshoot effect in wind-generated waves. *J. Geophys. Res.*, **73,** 6879–6885.

Dungey, J. C., and W. H. Hui, 1979: Nonlinear energy transfer in a narrow gravity-wave spectrum. *Proc. Roy. Soc. London,* **A368,** 239–265.

Fox, M. J. H., 1976: On the nonlinear transfer of energy in the peak of a gravity-wave spectrum, II. *Proc. Roy. Soc. London,* **A348,** 467–483.

Günther, H., W. Rosenthal and M. Dunckel, 1981: Directional wave spectra observed during JONSWAP 1973. *J. Phys. Oceanogr.*, **11,** 718–728.

Hasselmann, D. E., M. Dunckel and J. A. Ewing, 1980: Directional wave spectra observed during JONSWAP 1973. *J. Phys. Oceanogr.*, **10,** 1264–1280.

Hasselmann, K., 1961: On the nonlinear energy transfer in a gravity-wave spectrum. Part 1: General theory. *J. Fluid Mech.*, **12,** 481–500.

——, 1963: On the nonlinear energy transfer in a gravity-wave spectrum. Part 2: Conservation theorems; wave-particle analogy; irreversibility. *J. Fluid Mech.*, **15,** 273–281.

——, 1974: On the spectral dissipation of ocean waves due to white capping. *Bound. Layer Meteor.* **6,** 107–127.

——, T. P. Barnett, E. Bouws, H. Carlson, D. E. Cartwright, K. Enke, J. A. Ewing, H. Gienapp, D. E. Hasselmann, P. Kruseman, A. Meerburg, P. Muller, D. J. Olbers, K. Richter, W. Sell and H. Walden, 1973: Measurements of wind-wave growth and swell decay during the Joint North Sea Wave Project (JONSWAP). *Dtsch. Hydrogr. Z.,* **A8**(12), 95 pp.

——, D. B. Ross, P. Muller and W. Sell, 1976: A parametric wave prediction model. *J. Phys. Oceanogr.*, **6,** 200–228.

Hasselmann, S., and K. Hasselmann, 1981: *A Symmetrical Method of Computing the Nonlinear Transfer in a Gravity-Wave Spectrum.* Hamburger Geophys. Einzelschr., Reihe A., Wiss. Abh., **52,** 163 pp.

——, and ——, 1984: The wave model EXACT-NL. *Ocean Wave Modelling, The SWAMP Group,* Plenum Press, 249–251.

——, and ——, 1985: Computations and parameterizations of the nonlinear energy transfer in a gravity wave spectrum. Part I: A new method for efficient computations of the exact nonlinear transfer integral. *J. Phys. Oceanogr.*, **15,** 1369–1377.

——, ——, J. H. Allender and T. P. Barnett, 1985: Computations and parameterizations of the nonlinear energy transfer in a gravity wave spectrum. Part II: Parameterizations of the nonlinear energy transfer for application in wave models. *J. Phys. Oceanogr.*, **15,** 1378–1391.

——, K. Hasselmann, G. J. Komen, P. Jansen, J. A. Ewing and V. Cardone, 1987: The WAM model, a third generation ocean wave prediction model, (in preparation).

Janssen, P. A. E. M., and G. J. Komen, 1984: Effect of atmospheric stability on the growth of surface waves. *Bound.-Layer Meteor.*, **32,** 85–96.

Kitaigorodskii, S. A., 1983: On the theory of the equilibrium range in the spectrum of wind-generated gravity waves. *J. Phys. Oceanogr.*, **13,** 816–827.

Komen, G. J., S. Hasselmann and K. Hasselmann, 1984: On the existence of a fully developed wind-sea spectrum. *J. Phys. Oceanogr.*, **14,** 1271–1285.

Longuet-Higgins, M. S., 1976: On the nonlinear transfer of energy in the peak of a gravity-wave spectrum. *Proc. Roy. Soc. London,* **A347,** 311–328.

Masuda, A., 1980: Nonlinear energy transfer between wind waves. *J. Phys. Oceanogr.*, **10,** 2082–2093.

Miles, J. W., 1959: On the generation of surface waves by shear flows. Part 2. *J. Fluid Mech.*, **6,** 568–582.

Mitsuyasu, H., 1968a: On the growth of the spectrum of wind-generated waves. 1. **16,** 459–465.

——, 1968b: A note on the nonlinear energy transfer in the spectrum of wind-generated waves. *Rep. Res. Inst. Appl. Mech., Kyushu Univ.,* **16,** 251–264.

——, 1969: On the growth of the spectrum of wind-generated waves. 2. *Rep. Res. Inst. Appl. Mech., Kyushu Univ.,* **17,** 235–243.

——, and T. Honda, 1982: Wind induced growth of water waves. *J. Fluid. Mech.*, **123,** 425–442.

Phillips, O. M., 1957: On the generation of waves by turbulent wind. *J. Fluid. Mech.*, **2,** 417–445.

Pierson, W. J., 1964: The interpretation of wave spectrums in terms of the wind profile instead of the wind generated at a constant height. *J. Geophys. Res.*, **69,** 5191–5203.

——, and L. Moskowitz, 1964: A proposed spectral form for fully developed wind seas based on the similarity theory of S. A. Kitaigorodskii. *J. Geophys. Res.*, **69,** 5181–5190.

Sell, W., and K. Hasselmann, 1972: Computations of nonlinear energy transfer for JONSWAP and empirical wind-wave spectra. Rep. Institute of Geophysics, University of Hamburg.

Snyder, R. L., F. W. Dobson, J. A. Elliott and R. B. Long, 1981: Array measurements of atmospheric pressure fluctuations above surface gravity waves. *J. Fluid Mech.*, **102,** 1–59.

The SWAMP GROUP, 1985: *Ocean Wave Modeling,* Plenum Press, 256 pp.

Toba, Y., 1973: Local balance in the air–sea boundary processes. *J. Oceanogr. Soc. Japan,* **29,** 209–220.

Webb, D. J., 1978: Non-linear transfers between sea waves. *Deep-Sea Res.*, **25,** 279–298.

Young, I. R., and R. J. Sobey, 1985: Measurements of the wind-wave flux in an opposing wind, *J. Fluid Mech.*, **151,** 427–442.

——, S. Hasselmann and K. Hasselmann, 1985: Calculations of the nonlinear interactions in cross seas. *Hamburger Geophys. Einzelschriften, Heft* 74.

Zakharov, V. Y., and N. N. Filonenko, 1966: The energy spectrum for stochastic oscillations of a fluid surface. *Dokl. Akad. Nauk SSSR,* **170,** 1292–1295.

——, and M. M. Zaslavskii, 1982: The kinetic equation and Kolmogorov spectra in the weak turbulence theory of wind waves. *Izv., Atmos. Oceanic Phys.*, **18,** 747–753.